

Photoluminescence from Au ion-implanted nanoporous single-crystal $12\text{CaO}\cdot 7\text{Al}_2\text{O}_3$

Masashi Miyakawa,^{1,*} Hayato Kamioka,² Masahiro Hirano,¹ Toshio Kamiya,³ Peter V. Sushko,⁴ Alexander L. Shluger,⁴ Noriaki Matsunami,⁵ and Hideo Hosono^{1,3}

¹*Frontier Collaborative Research Center, Tokyo Institute of Technology, Mail Box S2-13, 4259 Nagatsuta, Midori-ku, Yokohama 226-8503, Japan*

²*Graduate School of Pure and Applied Sciences, University of Tsukuba, Tenodai 1-1-1, Tsukuba, Ibaraki 305-8571, Japan*

³*Materials and Structures Laboratory, Tokyo Institute of Technology, Mail Box R3-4, 4259 Nagatsuta, Midori-ku, Yokohama 226-8503, Japan*

⁴*Department of Physics and Astronomy, University College London, Gower Street, London WC1E 6BT, United Kingdom*

⁵*Division of Energy Science, EcoTopia Science Institute, Nagoya University, Furo-cho, Chikusa-ku, Nagoya 464-8603, Japan*
(Received 24 February 2006; published 12 May 2006)

Implantation of Au^+ ions into a single crystalline $12\text{CaO}\cdot 7\text{Al}_2\text{O}_3$ (C12A7) was performed at high temperatures with fluences from 1×10^{14} to $3 \times 10^{16} \text{ cm}^{-2}$. This material is composed of positively charged subnanometer-sized cages compensated by extra-framework negatively charged species. The depth profile of concentrations of Au species was analyzed using Rutherford backscattering spectrometry. The measured optical spectra and *ab initio* embedded cluster calculations show that the implanted Au species are stabilized in the form of negative Au^- ions below the fluences of $\sim 1 \times 10^{16} \text{ cm}^{-2}$ (Au volume concentration of $\sim 2 \times 10^{21} \text{ cm}^{-3}$). These ions are trapped in the cages and exhibit photoluminescence (PL) bands peaking at 3.05 and 2.34 eV at temperatures below 150 K. At fluences exceeding $\sim 3 \times 10^{16} \text{ cm}^{-2}$, the implanted Au atoms form nano-sized clusters. This is manifested in quenching of the PL bands and creation of an optical absorption band at 2.43 eV due to the surface plasmon of free carriers in the cluster. The PL bands are attributed to the charge transfer transitions ($\text{Au}^0 + e^- \rightarrow \text{Au}^-$) due to recombination of photo-excited electrons (e^-), transiently transferred by ultraviolet excitation into a nearby cages, with Au^0 atoms.

DOI: [10.1103/PhysRevB.73.205108](https://doi.org/10.1103/PhysRevB.73.205108)

PACS number(s): 78.55.-m, 78.20.Bh

I. INTRODUCTION

It has been recently demonstrated that a nano-porous complex oxide $12\text{CaO}\cdot 7\text{Al}_2\text{O}_3$ (C12A7) is capable of accommodating monovalent active anion species, such as H^- , O^- , and even electrons, at high concentrations unreachable at many conventional conditions.¹⁻³ The formation of these interstitial anions in C12A7 results from its characteristic crystal structure.⁴ C12A7 consists of a positively charged lattice framework ($[\text{Ca}_{24}\text{Al}_{28}\text{O}_{64}]^{4+}$), involving 12 cages per cubic unit cell and two extra-framework oxygen ions O^{2-} (called free oxygen ions hereafter), which occupy two different cages to compensate the positive charge of the framework. Using an appropriate chemical treatment one can replace the free oxygen ions with monovalent anions whose ionic sizes are smaller than the inner space of the cage ($\sim 0.4 \text{ nm}$). In addition to the chemical processes, we have found that the irradiation of C12A7 with energetic inert gas ions, such as Ar^+ and Xe^+ , at high temperatures can kick the free O^{2-} ions out of the lattice, leaving trapped electrons behind. This process neither destroys the lattice framework structure nor creates noticeable defects in the lattice, which may act as emission centers, for irradiation dose as high as 500 dpa.⁵ Therefore, we expect that heavymetal ions (M^-) with ionic sizes comparable to the cage space can also be formed in the C12A7 cages by hot implantation of M^+ ions in the presence of an electron source. This would correspond to the reaction $2\text{M}^+ + \text{O}^{2-}(\text{cage}) + 2e^-(\text{earth}) \rightarrow 2\text{M}^-(\text{cage}) + 1/2\text{O}_2(\text{gas})$, where two M^- ions occupy two different cages. This process could form a large amount of heavy metal anions at the surface and/or inside the bulk of C12A7, which would provide a

new insight into the entrapped state of anions in C12A7 as well as an opportunity for applications of heavy metal anions to emerging technological fields such as low temperature oxidation of methane.^{6,7}

In this study we selected Au^+ ions for hot implantation due to several reasons: (i) We expect that this may lead to formation of Au^- ions in C12A7 cages because the size of Au^- (0.366 nm)⁸ is comparable to that of the cage; (ii) Au^- ions substituting anions in alkali halides⁹⁻¹¹ are known to exhibit an efficient photoluminescence (PL) associated with the $6s^1 6p^1 \rightarrow 6s^2$ intra-ionic transition and it would be interesting to see whether an additional luminescence channel could be observed in C12A7 due to its complex structure of the conduction band; (iii) gold anion species [Au^- or $(\text{Au}_n)^-$] supported on oxide surfaces are expected to exhibit unique catalytic activities for oxidation reactions,¹²⁻¹⁸ in particular a catalytic role in the formation of CO_2 from CO at low temperatures.^{17,19} As we show below, using the optimized conditions we have succeeded in incorporating Au^- ions in the cages of C12A7 by the implantation of Au^+ ions. When irradiated with 3.8 eV photons, Au^- ions exhibit a characteristic PL at low temperatures, which we assign to the charge transfer transition of $\text{Au}^0 + e^- \rightarrow \text{Au}^-$ with the aid of the *ab initio* calculations. This PL channel is excited at much lower photon energies than, for example, intra-ionic Au^- luminescence in alkali halides due to a more complex electronic structure of C12A7 where the cage conduction band states are located below the excited $6s^1 6p^1$ state of Au^- . The excitation and PL energies associated with intra-atomic Au^- transitions, which could be observed at higher excitation energies, are also predicted.

II. EXPERIMENTAL PROCEDURES AND THEORETICAL ANALYSIS

C12A7 single crystals, grown by a floating zone method,²⁰ were sliced into ~ 1 mm thick plates and both surfaces were mirror-polished mechanically. The specimen was then heated to 600 °C and Au⁺ ions were implanted with an acceleration voltage of 300 kV. The fluence was varied from 1×10^{14} to 3×10^{16} cm⁻² with a constant dose rate of $\sim 3 \times 10^{12}$ cm⁻² s⁻¹ (~ 0.5 μ A cm⁻²). The depth concentrations of Au in the implanted samples were measured by the Rutherford backscattering spectrometry (RBS) using 1.8 MeV He⁺ ions. Optical absorption spectra were obtained by a conventional visible-ultraviolet (VIS/UV) and a Fourier transform infrared (IR) spectrophotometers at room temperature (RT). PL spectra were taken in the temperature range 6 K to RT using a He-Cd laser (325 nm) as an excitation source. PL lifetimes were measured at 20 K by a streak camera using a Nd-YAG laser (4ω :266 nm, ~ 2 ns) or a Ti:sapphire laser (3ω :266 nm, ~ 100 fs) as an excitation source.

The electronic structure of incorporated Au⁻ ions and their stability with respect to other possible extra-framework species were calculated using an embedded cluster approach implemented in the computer code GUESS.²¹ In this method the C12A7 was represented with a large nano-cluster (NC) containing ~ 7500 atoms. A “region of interest” including a defect and surrounding lattice atoms at the center of the NC was described quantum-mechanically (QM cluster) using the density functional theory (DFT) and the B3LYP density functional as implemented in the GAUSSIAN98 package.²² The remaining part of the system and its interaction with the QM cluster were described using classical inter-atomic potentials.²³ The total energy of the system was minimized with respect to the coordinates of ~ 500 quantum and classical atoms located within 12 Å from the center of the NC. This method allows us to account self-consistently for the defect-induced lattice relaxation and for the effect of this relaxation on the defect properties.²⁴ A more detailed description of the method is given elsewhere.²⁵ Two types of QM clusters containing, respectively, one and two adjacent framework cages were used in this work. Standard 6-31G basis set for quantum-mechanical O atoms was used, while Ca, Al, and Au atoms were represented using corresponding LANL2DZ basis sets. To investigate the stability of Au species in C12A7 we have calculated the total energies of the QM clusters containing several different extra-framework species, including Au⁺, Au⁰, Au⁻, and also O²⁻, O⁻, and e⁻ were calculated. The optical absorption energies for Au⁰ and Au⁻ have been calculated using time-dependent DFT approach.²² For comparison, we also calculated the excitation and the PL energies for Au⁻ in NaCl using the same embedded cluster approach and a cubic Na₁₃Cl₁₄ QM cluster.

III. RESULTS AND DISCUSSION

A. Formation of isolated Au⁻ ions and Au nano-clusters

Figure 1 shows depth profiles of concentrations of implanted Au obtained by RBS. The Au species has a peak at the depth of ~ 80 nm from the top surface and the position of

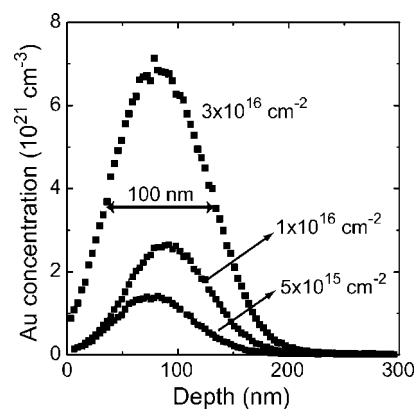


FIG. 1. Depth profiles of Au concentration in the C12A7 single crystals implanted with Au⁺ ion at various fluences.

this peak shifts deeper inside the sample as the fluence increases. Further, the peak height increases with the fluence, accompanied by broadening of the full width at the half maximum (FWHM). The peak positions, FWHM, and total Au concentrations as a function of fluence are summarized in Table I. Provided that each free oxygen ion can be replaced by two Au⁻ ions, the theoretical maximum concentration of monovalent anions accommodated in the C12A7 cages should be 2.33×10^{21} cm⁻³. As one can see in Table I, this concentration is provided by the Au⁺ implantation fluence of $\sim 1 \times 10^{16}$ cm⁻². It turns out that Au⁻ ions can be formed in C12A7 for the fluence, at least, below $\sim 1 \times 10^{16}$ cm⁻².

Figure 2 shows the change in the optical absorption due to the Au⁺-implantation of C12A7 crystals at fluences of 1×10^{15} , 1×10^{16} , and 3×10^{16} cm⁻². At low fluences (1×10^{15} cm⁻²) only a low-intensity absorption appears above ~ 3 eV. As the fluence increases to 1×10^{16} cm⁻², a broad featureless absorption band develops above ~ 2 eV. We also note that no noticeable absorption peaks attributable to Au clusters²⁷ were detected at these fluences. Finally, at higher fluence yet (3×10^{16} cm⁻²) the intensity of this broad band increases dramatically and a distinct absorption peak at 2.43 eV becomes obvious. The optical absorption due to RT-stable color centers (defects), i.e., Al-oxygen hole centers,²⁶ which were often induced by ion bombardments into aluminate crystals, is not observed in the hot implanted samples. Even if small amounts of the defects, hard to detect by the optical absorption, were induced, they do not exhibit PL. Further, when C12A7 was implanted with 300 kV Ar⁺ at 600 °C to 1×10^{16} to 1×10^{17} cm⁻², no PL was observed under the similar implanted condition.

TABLE I. Peak position, full width at half-maximum (FWHM), and total Au concentration in the C12A7 single crystals with various fluences of Au⁺ ion.

Fluence (cm ⁻²)	Peak position (nm)	FWHM (nm)	Concentration	
			Area (cm ⁻²)	Volume (cm ⁻³)
1×10^{15}	—	—	(2.8×10^{15})	(2.8×10^{20})
5×10^{15}	78	77	1.3×10^{16}	1.7×10^{21}
1×10^{16}	80	83	2.5×10^{16}	3.0×10^{21}
3×10^{16}	89	100	7.4×10^{16}	7.4×10^{21}

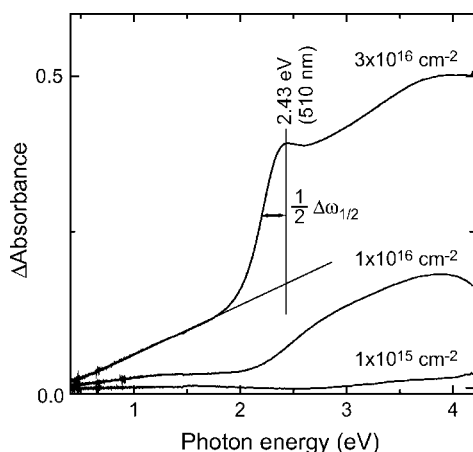
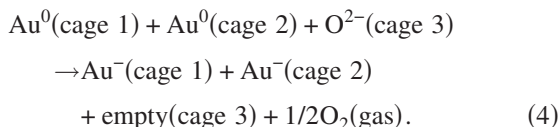
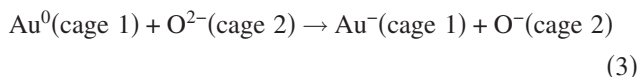
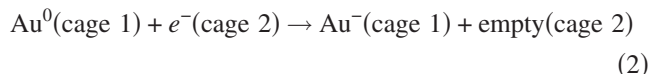
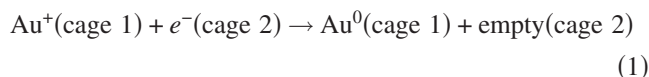


FIG. 2. Differences in optical absorption spectra of C12A7 crystals before and after Au^+ -implantation at various fluences.

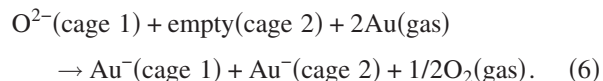
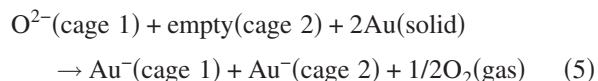
In order to understand the nature of these changes we considered the stability of different extra-framework species formed during the implantation. For that we calculated theoretically the enthalpy differences for the following reactions that are expected to take place during the implantation process in the limit of low concentration of Au species so agglomerates of gold atoms are not formed.



The implantation of Au^+ ions inevitably leads to formation of electron-hole pairs. Since the sample holder is kept at

the earth potential during the entire experiment, we presume that the holes leave the sample through it. The electrons remain in the system; they relax to occupy the lowest C12A7 conduction band formed by s -like states associated with cages unoccupied by atomic species (cage conduction band). These electrons readily combine with implanted Au^+ ions to form Au^0 atoms according to the reaction (1) with the enthalpy difference of -4.6 eV. Then, the Au^0 atoms can be converted to Au^- ions either via recombination with other electrons coming from the electron-hole pairs, as in reaction (2), or via charge-transfer, as in reaction (3), with the calculated enthalpy differences of -3.5 and -3.2 eV, respectively. Alternatively, Au^0 atoms can be converted to Au^- ions with simultaneous release of O_2 gas, as in reaction (4), with the enthalpy difference of -3.0 eV.

Other possible references for the relative energies of Au^- species could be solid and gas-phase gold:



The calculated enthalpy for reaction (5), which is a simple exchange process between Au atoms in solid gold and O^{2-} in the cage to form the Au^- in the cage, is estimated to be $+2.4$ eV. Positive enthalpy value makes the formation of Au^- through the reaction (5) unfavorable. However, similar reaction becomes favorable with respect to the gas-phase Au, as shown in reaction (6), with the estimated enthalpy change of -4.0 eV, which indicates that a significant amount of isolated Au species can be incorporated in C12A7.

The negative enthalpies of reactions (1)–(4) suggest that at low Au^+ fluence ($1 \times 10^{15} \text{ cm}^{-2}$) both Au^- and O^- species are stable in C12A7. The experimental data²⁸ and theoretical calculations predict that extra-framework O^- species induce weak optical absorption at ~ 3.0 eV and above, which corresponds to the electronic transitions from the top of the valence band (VB) to the unoccupied $2p$ level of O^- . Furthermore, our calculations show (see Table II) that Au^- can be photo-ionized by photons of 3.9 – 4.0 eV. Both findings are consistent with the observed weak absorption band shown in

TABLE II. Maxima of optical absorption and emission bands assigned to s – p electronic transitions of Au^- ions in alkali-halides. Energies taken from Refs. 9 and 10 are experimental ones. Calculated s – p intra-ionic transitions and charge transfer transitions of Au^- in C12A7 and NaCl are also shown. Energies are given in eV units.

	$s^2 \leftrightarrow sp$ transition			$\text{Au}^- \leftrightarrow \text{Au}^0 + e^-$		
	Experimental			Calculation		
	NaCl	KCl	KBr	NaCl	C12A7	C12A7
$S \rightarrow T$ (absorption)	4.23	4.07	4.00	4.5	4.2	3.9
$T \rightarrow S$ (emission)	4.1	3.95	3.89	4.1	3.8	2.0
$S \rightarrow S$ (absorption)	5.61	5.43	5.27	5.5	4.9–5.1	4.0
$S \rightarrow S$ (emission)	4.95	5.05	4.9	5.1	4.7	

Fig. 2. Moreover, the stability of the negatively charged Au^- ions is consistent with the positively charged framework.²⁹

At higher fluences ($1 \times 10^{16} \text{ cm}^{-2}$), when the bulk Au concentration ($\sim 3 \times 10^{21} \text{ cm}^{-3}$, see Table I) is larger than the maximum possible concentration of monovalent anions but still smaller than the concentration of cages ($\sim 7 \times 10^{21} \text{ cm}^{-3}$), formation of isolated Au^0 atoms becomes possible. Our calculations suggest that neutral Au^0 atoms induce additional optical absorption at 1.9 eV and above, which corresponds to the transitions from C12A7 VB to the unoccupied level of Au atom 6s state (see also Fig. 2). In addition, coexistence of Au^0 and Au^- gives rise to a charge transfer transition between these species at 0.6 eV.

Finally, at higher fluences yet ($3 \times 10^{16} \text{ cm}^{-2}$), the bulk Au concentration exceeds the concentration of framework cages. As a result, Au clusters (solid gold) become more stable than isolated Au atoms or ions. Indeed, with an increase in the fluence, a distinct absorption band peaking at $\sim 2.43 \text{ eV}$ appears (see Fig. 2) at the fluence of $3 \times 10^{16} \text{ cm}^{-2}$, which may be attributed to Au clusters. When a radius of a metal cluster (R) is less than the mean free path of free electrons in bulk metal, R is related to the plasmon absorption bandwidth at the half-maximum ($\Delta\omega_{1/2}$) by the following equation:³⁰

$$R = v_f / \Delta\omega_{1/2}. \quad (7)$$

Using the bulk value of Fermi velocity (v_f) of Au ($1.39 \times 10^8 \text{ cm s}^{-1}$), and the observed value for $\Delta\omega_{1/2}$ (0.46 eV), R is estimated to be $\sim 4 \text{ nm}$ for the fluence of $3 \times 10^{16} \text{ cm}^{-2}$. Further, the volume concentration of Au species in this sample is $\sim 7.4 \times 10^{21} \text{ cm}^{-3}$, which exceeds the total cage concentration ($6.99 \times 10^{21} \text{ cm}^{-3}$) in the C12A7. Based on these facts, it is reasonable to consider that the absorption band at 2.43 eV is due to the surface plasmon absorption and that the Au clusters start to form at the fluence of $3 \times 10^{16} \text{ cm}^{-2}$. Additionally, we observe that the differential absorbance above the peak energy increases approximately proportionally to the photon energy, suggesting that the absorption and/or transmission loss in this region is caused by the Mie scattering due to the Au particles that increases inversely proportional to the wavelength.³¹ The transmission loss due to the Mie scattering is reduced with a decrease in the fluence, supporting our assertion that the Au clusters contribute to the Mie scattering.

Therefore, we conclude that the final state of the implanted Au^+ ion in C12A7 varies depending on the implanted dose: Isolated Au^- ions are formed in the cages at low Au concentrations. At medium Au concentrations, where the concentration of Au exceeds the maximum concentration of monovalent ions (four ions in a unit cell) but is still less than the total cage number (12 cages in a unit cell), both Au^- and Au^0 can coexist. In the higher concentration region, Au starts to form clusters at the volume concentration of $\sim 7 \times 10^{21} \text{ cm}^{-3}$, which corresponds to the total cage concentration in the framework. The cluster formation is likely to be accompanied by a local damage of the C12A7 lattice framework, although the details of the Au cluster structure are unclear.

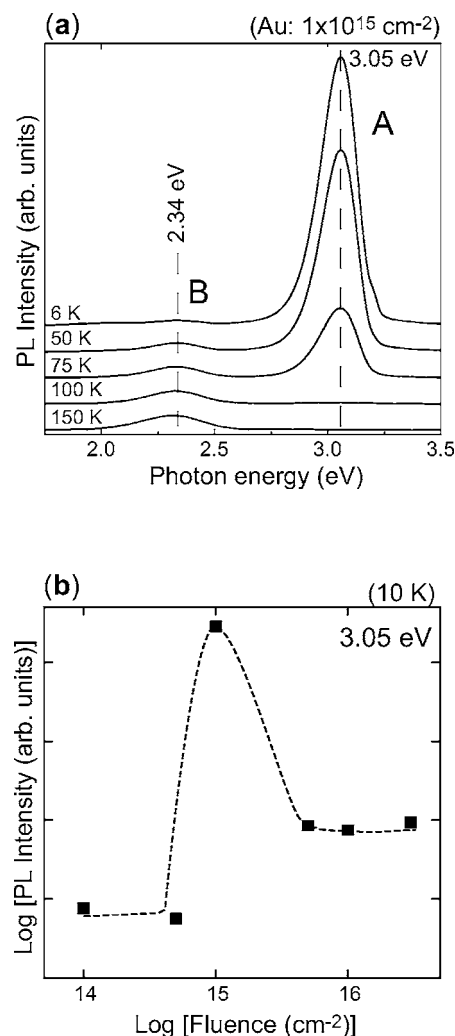


FIG. 3. Photoluminescence (PL) of Au^- ion in C12A7. (a) PL spectra of C12A7 single crystal implanted with Au^+ ions at a fluence of $\sim 10^{15} \text{ cm}^{-2}$ at temperatures from 6 to 150 K. (b) PL intensity of the 3.05 eV band at 10 K as a function of the Au^+ ion fluence.

B. Photoluminescence

The measured PL spectra and PL lifetimes of the C12A7 implanted at the fluence of $1 \times 10^{15} \text{ cm}^{-2}$, where the incorporated Au species are isolated, further confirm the formation of Au^- ions in C12A7. Irradiation of these samples with 3.8 eV photons induce an intense emission band peaking at 3.05 eV (A band) and a weak emission band at 2.34 eV (B band) readily observed at temperatures below 150 K, as shown in Fig. 3(a). With increasing the temperature, the PL intensity of the A band decreased, while that of the B band increased. The PL lifetimes were respectively $\sim 0.5 \text{ ns}$ for the A band and $\sim 130 \text{ ns}$ for the B band at 20 K.³² The PL intensity depends strongly on the Au concentration, exhibiting a sharp maximum at the fluence of $1 \times 10^{15} \text{ cm}^{-2}$ as shown in Fig. 3(b), which strongly suggests that the PL bands are associated with the Au^- , and the abrupt drop of the PL intensity with further increase in the fluence is explained tentatively by the onset of concentration quenching. At

higher implanted fluences, the formation of Au^0 atoms and Au clusters, which may result in the reduction of Au^- number and the energy transfer from the excited Au^- to surface plasmon of the cluster, becomes a dominant factor for the PL intensity reduction.

The larger band intensity and the shorter lifetime of the A band than those of the B band suggest that the A band is associated with an allowed transition, while the B band is with a forbidden one. This situation is similar to that of the Au^- centers in alkali-halides, where two emission bands are caused by the allowed singlet-singlet (*S-S*) and forbidden triplet-singlet (*T-S*) transitions of intra-atomic $6s^1 6p^1 \rightarrow 6s^2$, respectively. However, the observed PL energies in C12A7 are significantly smaller than those in alkali halides (see Table II). Further, our theoretical calculations indicate that the PL energies excited by the intra-ionic transitions of Au^- in C12A7 should be close to those in alkali halides, i.e., are much larger than the observed ones. (For comparison in Table II we also report the intra-ionic transition energies for Au^- in NaCl calculated the same embedded cluster approach.) Therefore, other possible transitions responsible for the observed PL bands in the Au implanted C12A7 have to be considered.

Figure 4(a) shows the local atomic structure of an Au^- ion in a C12A7 cage calculated using the embedded cluster approach. Since the size of an Au^- ion is comparable to the cage inner space, the cage wall deforms slightly and expands so as the distance between two Ca ions along the cage S_4 axis (D_{S_4}) increases by approximately 0.007 nm ($\sim 1.2\%$ of the cage inner size) with respect to the empty cage, resulting in 0.568 nm. The deformation is much smaller than those caused by the free O^{2-} ions ($D_{S_4} = 0.442$ nm)³³ and electrons ($D_{S_4} = 0.499$ nm).²⁴

The one-electron energy levels of Au^- in C12A7, calculated using the two-cage QM cluster by taking the deformation into consideration, are shown in the left side of Fig. 4(b). The $6s^2$ state of Au^- ion is located in the band gap approximately 1.4 eV above the valence band and ~ 4.5 eV below the lowest unoccupied state, which also provides a distinct confirmation for the stability of the Au^- in the cage. The interaction between one-electron states associated with unoccupied cages gives rise to the cage conduction band (CCB).^{25,34} Formation of such a band is unique for C12A7 in which each sub-nanometer-sized cage is connected to eight nearest-neighbor cages to form a three-dimensional network structure. The $6p$ states of Au^- are just below the higher conduction band originating from the states of the framework cations (framework conduction band).

The calculated values of the excitation energies of intra-atomic $6s^2 \rightarrow 6s^1 6p^1$ singlet-singlet (*S-S*) and singlet-triplet (*S-T*) transitions calculated using TDDFT are ~ 4.8 – 5.1 eV and ~ 4.1 – 4.3 eV, respectively (see also Table II). Thus, these transitions cannot be excited using the He-Cd laser light (~ 3.8 eV). However, this laser can induce the charge-transfer transition $\text{Au}^- + h\nu \rightarrow \text{Au}^0 + e^-$, in which Au^- ion is effectively photo-ionized and the photo-ionized electron is promoted to the cage conduction band and forms a polaron state.^{24,34} The polaron is then relaxed so as the excited electron localizes in a nearby cage either in the singlet or triplet

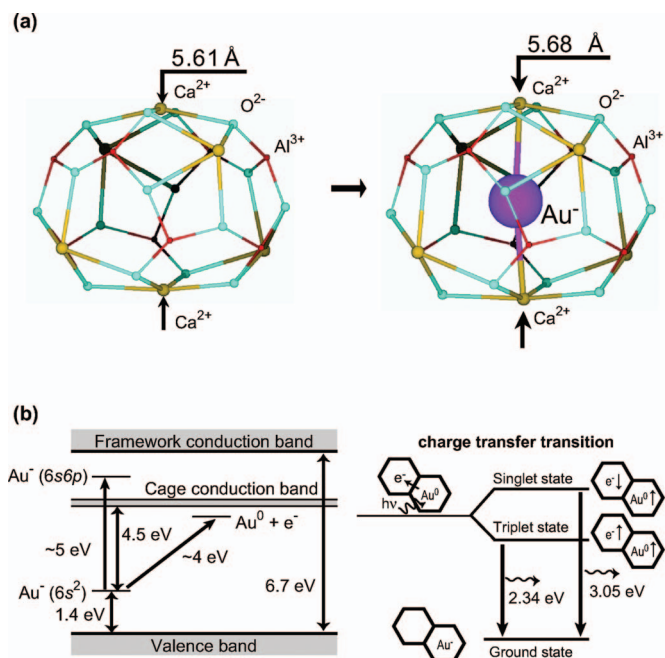


FIG. 4. (Color) Crystallographic cage structure and schematic energy diagram in Au^- ion accommodated C12A7. (a) Local atomic structure of an Au^- ion incorporated cage in C12A7 as calculated using the two-cage QM cluster. The Ca-Ca distance along the cage S_4 axis (D_{S_4}) is a measure for the cage wall distortion induced by the extra-framework species. (b) The left side shows energy levels of Au^- incorporated C12A7 calculated using the two-cage QM cluster (see text for details). The right side shows a diagram of the charge transfer transition responsible for the photoluminescence, where the 3.05 and 2.34 eV bands are, respectively, assigned to the $\text{Au}^0 + e^- \rightarrow \text{Au}^-$ transitions from the singlet and triplet states to the ground state. The hexagon represents a crystallographic cage in C12A7.

state depending on the direction of the spin moment of the electron, as shown in the right side of Fig. 4(b). The calculated values of the photo-ionization energies for the *S-S* and *S-T* transitions, also calculated using TDDFT, are 4.0 and 3.9 eV, respectively.

Then, the relaxation of the triplet excited state was considered in detail to estimate the PL energy: It involves mainly the cage occupied by the electron where the D_{S_4} decreases from 0.554 nm to ~ 0.5 nm. The energy of the *T-S* luminescent transition $\text{Au}^0 + e^- \rightarrow \text{Au}^-$, calculated as the difference of the triplet and singlet states for this configuration is ~ 2.0 eV, which is good agreement with the observed PL energy for B band, suggesting that B band is due to the *T-S* charge-transfer transition. We note that the Stokes shift for B band is significantly smaller than, for example, in the case of the photo-ionization of H^- in C12A7²⁵ because the large Au atom partially constrains the relaxation of the framework. Although the theoretical assignment of the A band remains unclear, the slightly higher energy and the much shorter PL life time of A band than those of B band strongly suggest that A band is assigned as the inter-cage *S-S* transition. This model also explains the temperature dependences of the PL intensities of A and B bands: The thermal relaxation from the singlet to triplet states is enhanced with increase of tempera-

ture, resulting in the increase in B band, and the corresponding decrease in A band with temperature. Further, faster lifetimes of both A and B bands than those of the PL bands of Au^- in alkali halides are likely attributed to the migration of the excited electrons to other cages (the electron drift in the cage conduction band). The decrease of the PL intensity at fluences higher than $\sim 10^{15} \text{ cm}^{-2}$ is due to the formation of an additional photo-excitation channel, which corresponds to the electron transfer from Au^- to an Au^0 , thus bypassing the CCB states. To summarize, the assignment of the PL bands as due to the charge transfer transitions of $\text{Au}^0 + e^- \rightarrow \text{Au}^-$, provides solid evidence that Au^- ions are incorporated in the cages of C12A7 by the hot Au^+ ion implantation at fluences of $\sim 10^{15} \text{ cm}^{-2}$.

The formation of a negative valence state of Au is likely to be due to a combined effect of the presence of the nano-sized cage structure and positively charged framework in C12A7. Indeed, PL bands attributable to Au^- ions were not detected in a compound $5\text{CaO} \cdot 3\text{Al}_2\text{O}_3$ (C5A3), which has a similar chemical composition with C12A7 but no nanoporous structure. Further, PL bands were detected neither in an Au^+ -implanted MgO single crystal, yttria-stabilized ZrO_2 single crystal, nor SiO_2 glass at the same fluence of $\sim 1 \times 10^{15} \text{ cm}^{-2}$. SiO_2 glass is known to have small voids, in which neutral species such as H_2O and O_2 molecules, can accommodate up to $\sim 10^{21} \text{ cm}^{-3}$,³⁵ but it does not have positively charged lattice capable of stabilizing negatively charged species or anions.

Finally, we should note that Au^- is the only encaged anion in C12A7 that exhibits photoluminescence among all encaged anions so far discovered. This may result from much smaller nonradiative relaxation probability than those of other anions entrapped in the cage that can exhibit PL when doped in other host. The ionic radius of the Au^- ion is very close to that of the cage, which reduces the distortion of the cage, leading to the decrease in the electron phonon (e - p)

interaction between the Au^- ion and the cage framework. For example, O_2^- ion which exhibits superradiance emission in alkali halides,³⁶ does not emit at all in C12A7 presumably because of the strong e - p interaction of the O_2^- ion in C12A7,³⁷ which induces a rapid depopulation of the excited state through the nonradiative relaxation process.

IV. CONCLUSIONS

We have successfully accommodated Au^- ions in the C12A7 cages by Au^+ ion implantation at 600 °C with a fluence of $\sim 1 \times 10^{15} \text{ cm}^{-2}$. The Au^- ion exhibits the photoluminescence bands at ~ 3.05 and ~ 2.34 eV at temperatures ≤ 150 K. These bands are attributed to the charge-transfer transition of $\text{Au}^0 + e^- \rightarrow \text{Au}^-$. At higher fluences, implanted Au^+ ions form Au nano-particles with a diameter of ~ 4 nm at high fluence implantation. These nano-particles show a plasmon absorption band peaking at ~ 2.43 eV. The C12A7 crystal containing Au^- ions, Au^0 atoms and/or Au nano-particles, with their concentrations controllable by the implantation fluence, provides a unique platform to investigate electronic and structural states of large anions encaged in nano-porous materials as well as to cultivate emerging applications specific to heavy metal anions such as catalyst.

ACKNOWLEDGMENTS

RBS measurements were conducted using KN Van de Graff Accelerator at Nagoya University. This work was supported by the Grant-in-Aid for Creative Scientific Research (Grant No. 16GS0205) from the Japanese Ministry of Education, Culture, Sports, Science, and Technology. The calculations were carried out on the UCL Central Computing Cluster C³. We would like to thank J. L. Gavartin and K. McKenna for their comments on the manuscript.

*Corresponding author. Telephone: +81-45-924-5127; FAX: +81-45-924-5127. Electronic address: m-miyakawa@lucid.msl.titech.ac.jp

¹K. Hayashi, M. Hirano, S. Matsuishi, and H. Hosono, *J. Am. Chem. Soc.* **124**, 738 (2002).

²S. Matsuishi, Y. Toda, M. Miyakawa, K. Hayashi, T. Kamiya, M. Hirano, I. Tanaka, and H. Hosono, *Science* **301**, 626 (2003).

³K. Hayashi, S. Matsuishi, T. Kamiya, M. Hirano, and H. Hosono, *Nature (London)* **419**, 462 (2002).

⁴H. Bartl and T. Scheller, *Neues Jahrb. Mineral., Monatsh.* **35**, 547 (1970).

⁵To our surprise, C12A7 crystal structure remains without converting amorphous state by such heavy ion bombardment exceeding 500 dpa: M. Miyakawa, Y. Toda, K. Hayashi, M. Hirano, T. Kamiya, N. Matsunami, and H. Hosono, *J. Appl. Phys.* **97**, 023510 (2005).

⁶I. Bar-Nahum, A. M. Khenkin, and R. Neumann, *J. Am. Chem. Soc.* **126**, 10237 (2004).

⁷M.-H. Baik, M. Newcomb, R. A. Friesner, and S. J. Lippard,

Chem. Rev. (Washington, D.C.) **103**, 2385 (2003).

⁸Ionic radius of Au^- ion ($r=0.188$ nm) is estimated from CsAu crystal. [G. A. Tinelli and D. F. Holcomb, *J. Solid State Chem.* **25**, 157 (1978).]

⁹F. Fischer, *Z. Phys.* **231**, 293 (1970); M. Krause and F. Fischer, *J. Lumin.* **4**, 335 (1971); A. Overberg and F. Fischer, *Phys. Status Solidi B* **147**, 811 (1988).

¹⁰K. Shigematsu and R. Onaka, *Sci. Light (Tokyo)* **23**, 27 (1974); H. Takezoe, *ibid.* **24**, 1 (1975).

¹¹P. W. M. Jacobs, *J. Phys. Chem. Solids* **52**, 35 (1991).

¹²M. Haruta, T. Kobayashi, H. Sano, and N. Yamada, *Chem. Lett.* **16**, 405 (1987); M. Haruta, N. Yamada, T. Kobayashi, and S. Iijima, *J. Catal.* **115**, 301 (1989).

¹³M. Haruta, *Catal. Today* **36**, 153 (1997).

¹⁴M. Valden, X. Lai, and D. W. Goodman, *Science* **281**, 1647 (1998).

¹⁵Q. Fu, H. Saltsburg, and Flytzani-Stephanopoulos, *Science* **301**, 935 (2003).

¹⁶J. Guzman and B. C. Gates, *J. Am. Chem. Soc.* **126**, 2672 (2004).

- ¹⁷Z. Yan, S. Chinta, A. A. Mohamed, J. P. Fackler, Jr., and D. W. Goodman, *J. Am. Chem. Soc.* **127**, 1604 (2005).
- ¹⁸J. Guzman, S. Carretin, and A. Corma, *J. Am. Chem. Soc.* **127**, 3286 (2005).
- ¹⁹H. Hakkinen and U. Landman, *J. Am. Chem. Soc.* **123**, 9704 (2001); L. D. Socaciu, J. Hagen, T. M. Bernhardt, L. Woste, U. Heiz, H. Hakkinen, and U. Landman, *ibid.* **125**, 10437 (2003).
- ²⁰S. Watauchi, I. Tanaka, K. Hayashi, M. Hirano, and H. Hosono, *J. Cryst. Growth* **237-239**, 801 (2002).
- ²¹P. V. Sushko, A. L. Shluger, and C. R. A. Catlow, *Surf. Sci.* **450**, 153 (2000).
- ²²GAUSSIAN 98 (Revision A.7), M. J. Frisch, G. W. Trucks, H. B. Schlegel, G. E. Scuseria, M. A. Robb, J. R. Cheeseman, V. G. Zakrzewski, J. A. Montgomery, Jr., R. E. Stratmann, J. C. Burant, S. Dapprich, J. M. Millam, A. D. Daniels, K. N. Kudin, M. C. Strain, O. Farkas, J. Tomasi, V. Barone, M. Cossi, R. Cammi, B. Mennucci, C. Pomelli, C. Adamo, S. Clifford, J. Ochterski, G. A. Petersson, P. Y. Ayala, Q. Cui, K. Morokuma, D. K. Malick, A. D. Rabuck, K. Raghavachari, J. B. Foresman, J. Cioslowski, J. V. Ortiz, A. G. Baboul, B. B. Stefanov, G. Liu, A. Liashenko, P. Piskorz, I. Komaromi, R. Gomperts, R. L. Martin, D. J. Fox, T. Keith, M. A. Al-Laham, C. Y. Peng, A. Nanayakkara, C. Gonzalez, M. Challacombe, P. M. W. Gill, B. Johnson, W. Chen, M. W. Wong, J. L. Andres, C. Gonzalez, M. Head-Gordon, E. S. Replogle, and J. A. Pople, Gaussian Inc., Pittsburgh, PA, USA, 1998.
- ²³M. O. Zacate and R. W. J. Grimes, *J. Phys. Chem. Solids* **63**, 675 (2002).
- ²⁴P. V. Sushko, A. L. Shluger, K. Hayashi, M. Hirano, and H. Hosono, *Phys. Rev. Lett.* **91**, 126401-1 (2003).
- ²⁵P. V. Sushko, A. L. Shluger, K. Hayashi, M. Hirano, and H. Hosono, *Phys. Rev. B* (to be published).
- ²⁶Although an absorption band of the Al-oxygen hole center in C12A7 glass was observed peaking at ~ 3.9 eV [H. Hosono, K. Yamazaki, and Y. Abe, *J. Am. Chem. Soc.* **70**, 867 (1987)], an observed weak band in this energy region in Fig. 3 is not attributable to the center, because no absorption band is induced at ~ 3.9 eV in the Ar⁺-implanted C12A7 film even at a high fluence of $\sim 10^{18}$ cm⁻². The band is most likely associated with the implanted Au.
- ²⁷R. H. Magruder III, L. Yang, R. F. Haglund, Jr., C. W. White, L. Yang, R. Dorsinville, and R. R. Alfano, *Appl. Phys. Lett.* **62**, 1730 (1993).
- ²⁸K. Hayashi, S. Matsuishi, M. Hirano, P. V. Sushko, A. L. Shluger, S. Watauchi, M. Yamanaka, I. Tanaka, H. Hosono, *J. Phys. Chem. B* (to be published).
- ²⁹T. Kamiya and H. Hosono, *Jpn. J. Appl. Phys., Part 1* **44**, 774 (2005).
- ³⁰W. T. Doyle, *Phys. Rev.* **111**, 1067 (1958); G. W. Arnold, *J. Appl. Phys.* **46**, 4466 (1975).
- ³¹G. Mie, *Ann. Phys.* **25**, 377 (1908).
- ³²H. Kamioka, M. Miyakawa, T. Kamiya, M. Hirano, and H. Hosono (in preparation).
- ³³P. V. Sushko, A. L. Shluger, K. Hayashi, M. Hirano, and H. Hosono, *Phys. Rev. B* (to be published).
- ³⁴P. V. Sushko, A. L. Shluger, K. Hayashi, M. Hirano, and H. Hosono, *Appl. Phys. Lett.* **86**, 092101-1 (2005).
- ³⁵R. H. Doremus, *Diffusion of Reactive Molecules in Solids and Melts* (Wiley, New York, 2002); K. Kajihara, M. Hirano, L. Skuja, and H. Hosono, *J. Appl. Phys.* **98**, 043515-1 (2005).
- ³⁶J. Rolfe, F. R. Lipsett, and W. J. King, *Phys. Rev.* **123**, 447 (1961); R. Florian, L. O. Schwan, and D. Schmid, *Solid State Commun.* **42**, 55 (1982).
- ³⁷S. Matsuishi, K. Hayashi, M. Hirano, I. Tanaka, and H. Hosono, *J. Phys. Chem. B* **108**, 18557 (2004).